# Supplemental materials for:

# A C9orf72-CARM1 Axis Regulates Lipid Metabolism Under Glucose Starvation-induced Nutrient Stress

Yang Liu[1,2], Tao Wang[1,2], Yon Ju Ji[1,2], Kenji Johnson[1,2], Honghe Liu[1,2], Kaitlin Johnson[1], Scott Bailey[1], Yongwon Suk[1,2], Yu-Ning Lu[1,2], Mingming Liu[1,2], Jiou Wang[1,2*]

Corresponding author: Jiou Wang, jiouw@jhu.edu

This file includes:

Supplemental Figures and Legends S1 to S7
Supplemental Tables S1 to S2

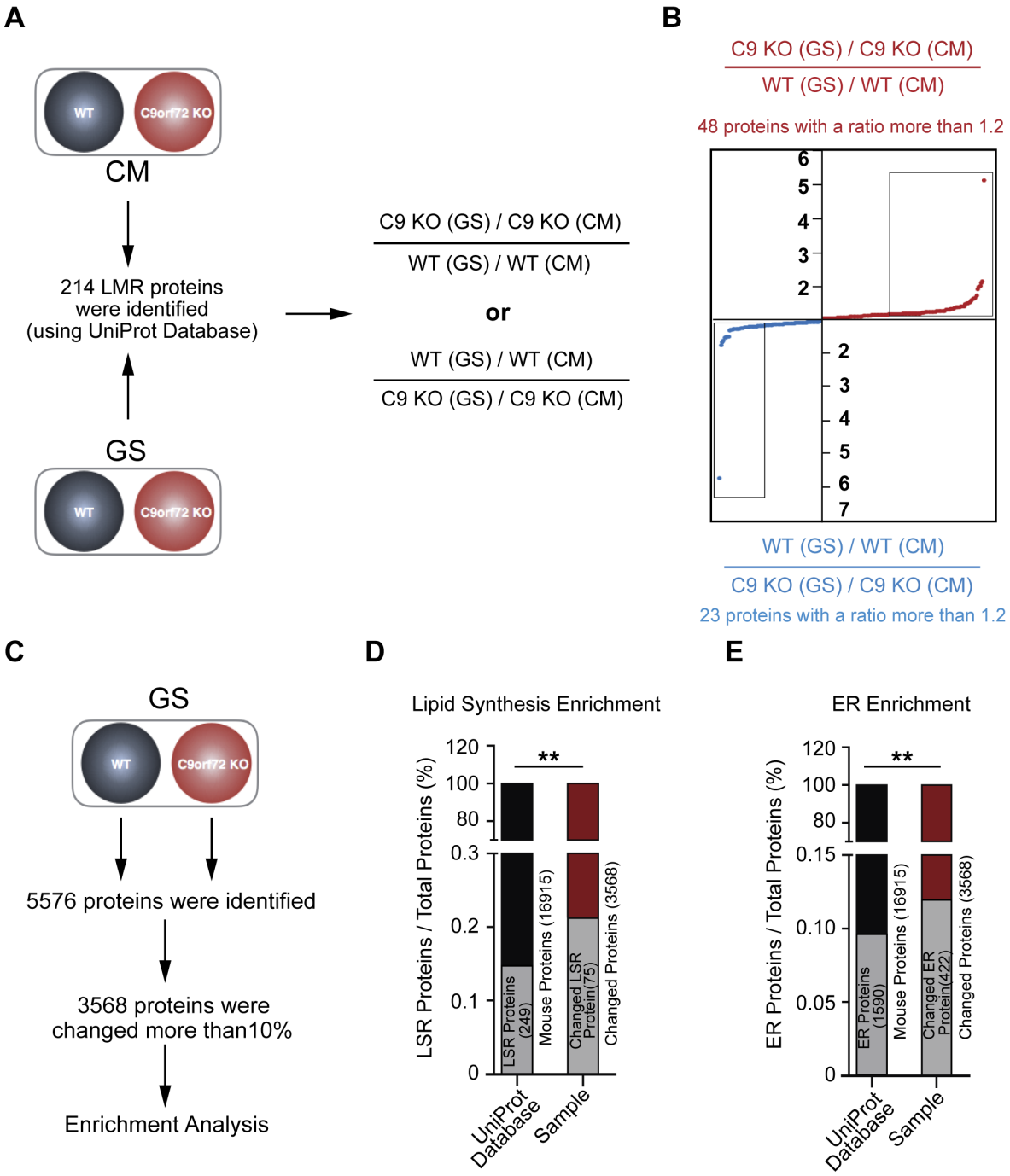


**Supplemental Figure S1. The proteomic analysis showing altered lipid metabolism under glucose starvation upon the loss of C9orf72.**

(A) The scheme of quantitative proteomic analysis. WT and C9orf72-/- MEFs were cultured with complete medium (CM) or treated with glucose starvation (GS) for 6 hours and then harvested for quantitative proteomic analysis. Ratios of C9orf72-/- (GS) / C9orf72 (CM) and WT (GS) / WT (CM) mean the extent of the protein amount variation induced by glucose starvation in C9orf72-/- and WT MEFs, respectively. Further comparison of the two ratios reflects the differential influence of glucose starvation on protein amounts, especially lipid

metabolism relative (LMR) proteins, which were identified using the UniProt database as described in methods. The further a ratio is from 1, the more change it indicates for the protein level as a result of glucose starvation in C9orf72-/- MEFs relative to WT cells; on the other hand, a ratio closer to 1 indicates that glucose starvation induces a similar change in the protein level in C9orf72-/- MEFs as in WT cells. (B) Glucose starvation induced upregulation of 48 LMR proteins and downregulation of 23 LMR proteins in C9orf72-/- MEFs relative to WT MEFs. (C) The scheme of enrichment analysis on the lipid biosynthetic process and the endoplasmic reticulum (ER) function using the quantitative proteomic data. Proteins that varied more than 10% were used in the enrichment analysis. (D and E) The enrichment of proteins on the lipid biosynthetic process and the endoplasmic reticulum (ER) function was analyzed by Fisher's test via comparing the proteomic data with the UniProt database. **$p < 0.01$.

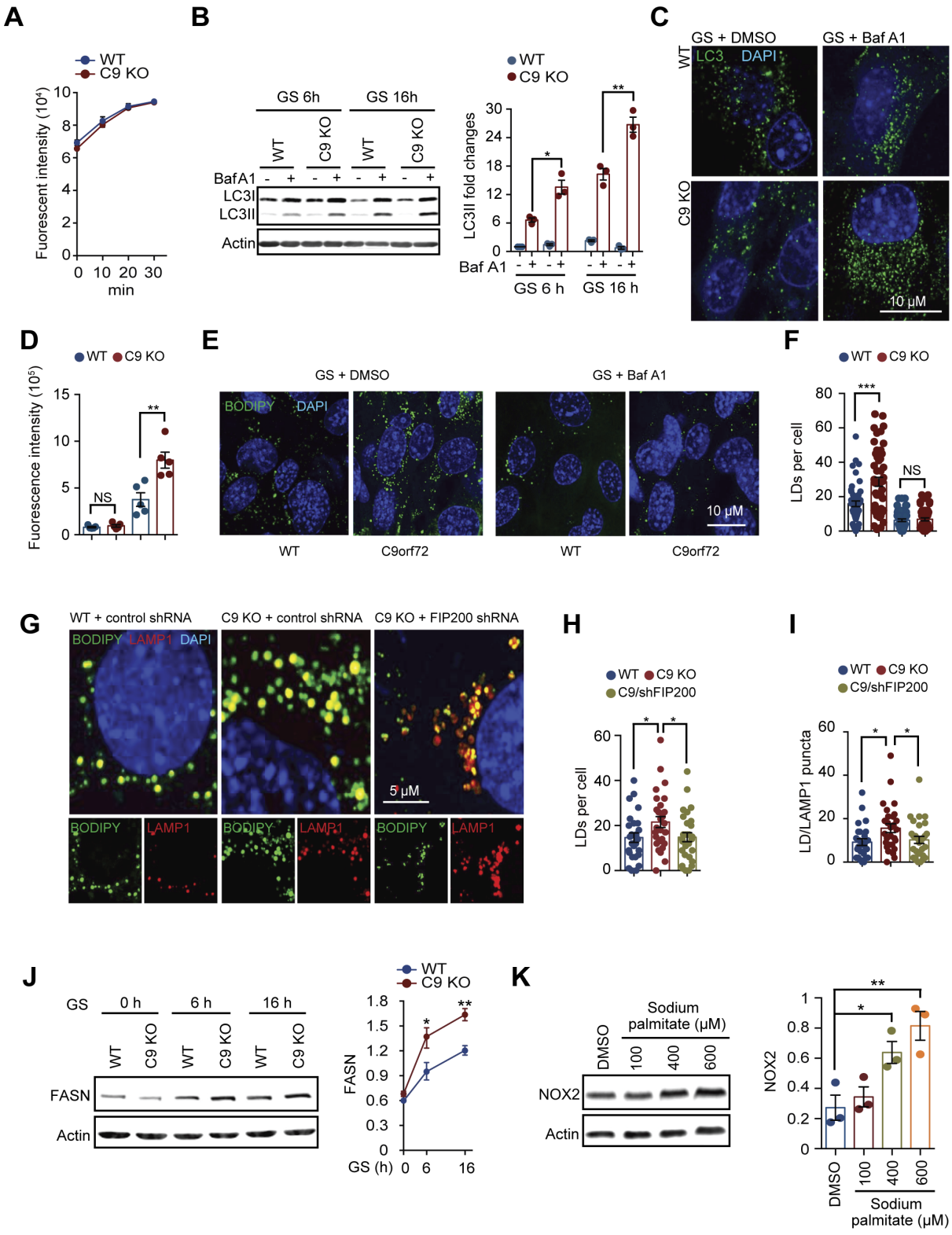


**Supplemental Figure S2. Increased autophagic flux contributes to dysfunctional lipid metabolism in the absence of C9orf72 upon glucose starvation.**

(A) WT and C9orf72 MEFs were starved with glucose free medium for 4 hours, then cultured with glucose- and serum-free medium for 1 hour. The rate of cellular FA uptake was then evaluated at 10-minute intervals for 30 minutes. (B) WT and C9orf72-/- MEFs were grown

under glucose starvation conditions for 6 and 16 hours in the presence of bafilomycin A1 (100 nM). The fold changes of LC3II were statistically analyzed. n=3. (C, D) WT and C9orf72-/- MEFs were grown under glucose starvation conditions for 6 hours with or without bafilomycin A1 (100 nM). Cells were then fixed and stained against the autophagosome marker LC3 II. LC3 immunofluorescence intensity per cell in 5 view fields containing 115-145 cells in each group was statistically analyzed. (D) WT and C9KO MEFs were cultured in glucose free medium with or without bafilomycin A1 (100 nM). LDs were labeled by BODIPY. (E and F) WT and C9KO cells were starved with glucose free medium for 16 hours with or without the presence of bafilomycin A1 (100 nM). LDs and autophagic digestion of LDs were labeled by BODIPY and BODIPY/LAMP1, and 50 cells from 3 independent experiments were statistically analyzed. (G-I) WT and C9KO MEFs were starved with glucose free medium for 6 and 16 hours, and the protein levels of FASN were determined by immunoblotting. n=3. (H) WT MEFs were cultured in glucose free medium with indicated concentrations of sodium palmitate for 16 hours. The protein levels of NOX2 were determined by immunoblotting. n=3. Complete Culture Medium (CM), Glucose Starvation (GS). Data are presented as mean ± SEM; *$p < 0.05$, **$p < 0.01$.

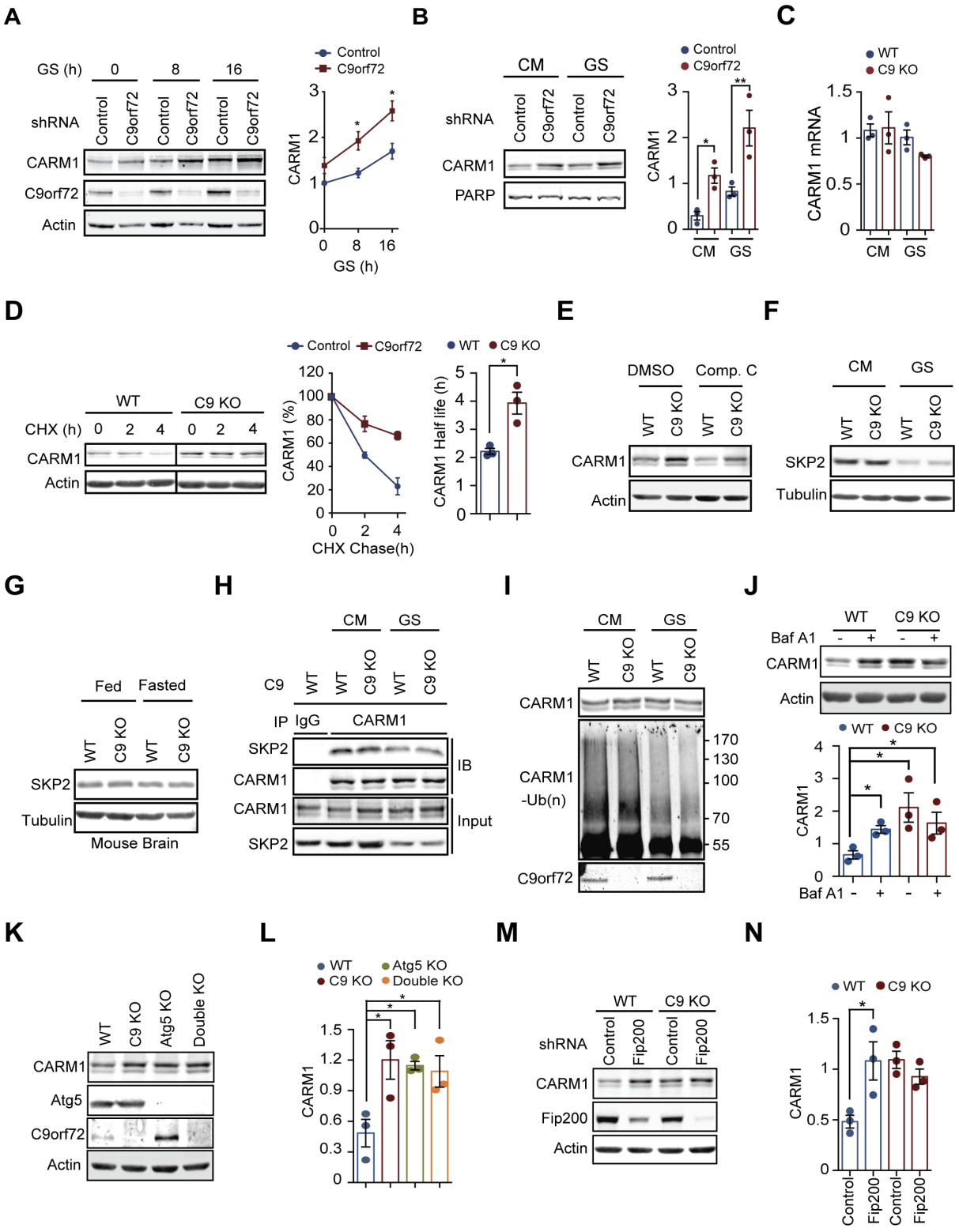


**Supplemental Figure S3. C9orf72 regulates the turnover of CARM1 protein.**

(A) HEK293 cells stably expressing a C9orf72-specific shRNA or a control shRNA were grown under glucose starvation conditions for 0 hour, 8 hours, and 16 hours. The protein levels of endogenous CARM1 and C9orf72 were determined by immunoblotting. n=3. (B). HEK293T cells stably expressing a C9orf72-specific shRNA or a control shRNA were grown

under glucose starvation conditions for 6 hours, and the nuclear fractions were separated. Endogenous CARM1 was analyzed by immunoblotting. n=3. (C) WT and C9orf72-/- MEFs were starved with glucose free medium for 6 hours, and CARM1 mRNA levels were determined by quantitative PCR. n=3. (D) WT and C9orf72-/- MEFs were grown under glucose starvation conditions in the presence of 10 μg/ml Cycloheximide (CHX). CARM1 protein levels were determined at each indicated time points after initial four hours of starvation. The half-life ($t_{1/2}$) of CARM1 protein was calculated. n=3. (E) WT and C9KO MEFs were cultured under glucose starvation conditions with DMSO or Compound C (10 μM) for 6 hours. CARM1 protein levels were detected by immunoblotting. (F) WT and C9orf72-/- MEFs were treated with or without glucose starvation for 6 hours, and SKP2 protein levels were determined by immunoblotting. SKP2 was reduced under glucose starvation, but the loss of C9orf72 did not change the SKP2 protein level. (G) WT and C9orf72-/- mice were fed or fasted for 24 hours, and the cerebral cortex tissues were analyzed for SKP2 protein levels with immunoblotting. (H) WT and C9orf72-/- MEFs were grown with or without glucose starvation conditions for 4 hours in the presence of MG132 (10 μM). Using whole cell lysates, immunoprecipitation was performed using an CARM1 antibody and an IgG isotope control, followed by immunoblotting analysis of SKP2 and CARM1. The loss of C9orf72 did not affect the binding of CARM1 to SKP2. (I) WT and C9orf72-/- MEFs were cultured with CM or glucose free medium in the presence of MG132 (10 μM) for 4 hours. Endogenous CARM1 was immunoprecipitated from the whole cell lysates, and the ubiquitinated CARM1 (CARM1-Ub(n)) was analyzed by immunoblotting with a ubiquitin antibody. The loss of C9orf72 did not affect the ubiquitination of CARM1. (J) WT and C9KO MEFs were cultured in glucose free medium in the absence or presence of bafilomycin A1 (100 nM). CARM1 protein levels were detected by immunoblotting. n=3. (K and L) WT, C9KO, Atg5KO, and C9/Atg5 double KO MEFs were starved with glucose free medium for 6 hours, and CARM1 protein levels were measured by western blotting. n=3. (M and N) WT and C9KO MEFs stably expressing control shRNA or FIP200 shRNA were cultured in glucose starvation conditions for 6 hours, and CARM1 protein levels were measured by western blotting. n=3. Complete Culture Medium (CM), Glucose Starvation (GS). Data are presented as mean ± SEM; *$p < 0.05$, **$p < 0.01$.

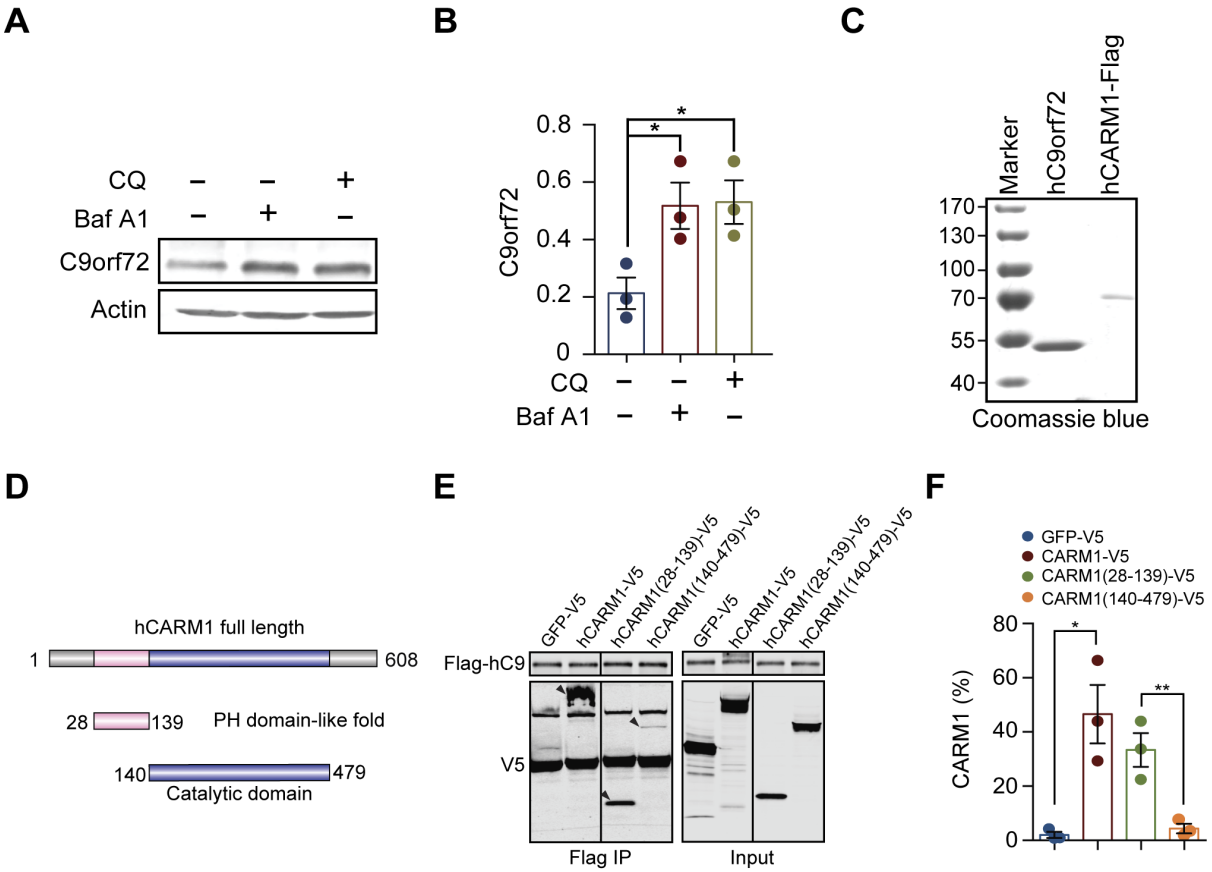


**Supplemental Figure S4. C9orf72 is increased by inhibiting lysosomal degradation and interacts with CARM1.**

(A and B) MEFs were cultured with the complete medium in the presence of the inhibitor of lysosomal degradation, bafilomycin A1 (100 nM) or Chloroquine (25 μM), and the levels of C9orf72 protein were analyzed by immunoblotting. n=3. (C) Purified proteins of hC9orf72 and hCARM1 were stained with Coomassie blue. (D) The protein domains of CARM1. (E and F) The full-length protein and the two structured domains (PH domain-like fold: 28-139, catalytic domain: 140-479) of V5-hCARM1 were expressed with Flag-hC9orf72 in HEK 293 cells. After cells were starved for 16 hours, immunoprecipitation was conducted using Flag beads. n=3. Data are presented as mean ± SEM; *p < 0.05, **p < 0.01.

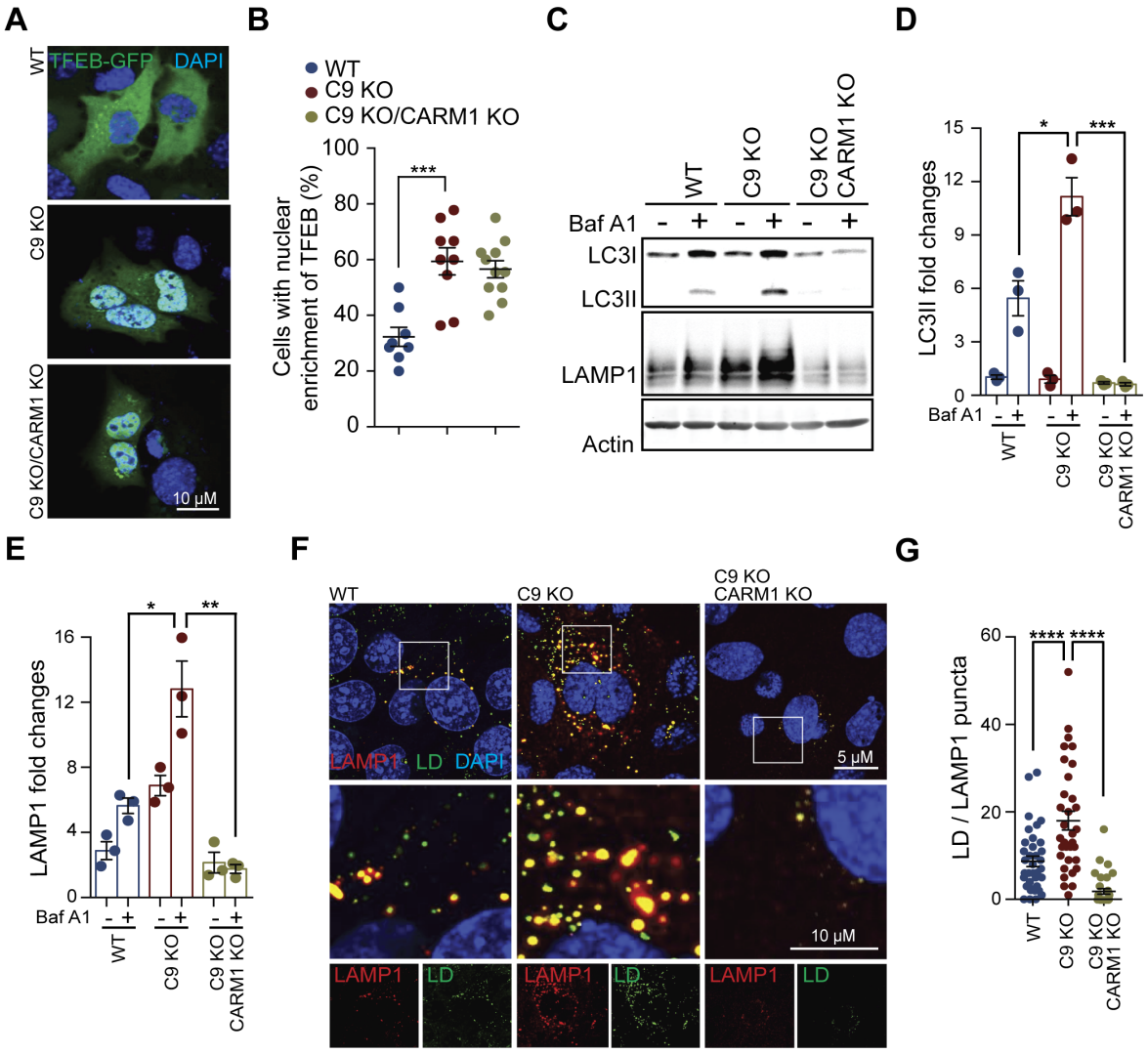


**Supplemental Figure S5. The deletion of CARM1 reverses the increase in the autophagic digestion of LDs caused by loss of C9orf72.**

(A and B) GFP-TFEB was expressed in WT, C9KO, and C9/CARM1 double KO MEFs starved with glucose free medium for 6 hours. 8-11 fields of view containing 45-86 cells were statistically analyzed for nuclear enrichment of GFP-TFEB. (C) WT, C9orf72-/-, and C9orf72/CAMR1 double knockout MEFs were grown under glucose starvation for 6 hours with or without the autophagy inhibitor bafilomycin A1 (100 nM). The autophagy marker LC3I/II and the lysosomal marker LAMP1 were analyzed by immunoblotting. (D and E) The fold changes of LC3II and LAMP1 protein levels were statistically analyzed. n=3. Loss of C9orf72 increased the autophagic flux, as indicated by the increase of LC3II in the presence of bafilomycin A1 that blocks the lysosomal turnover of LC3II, but the deletion of CARM1 reversed the effects caused by loss of C9orf72. Accordingly, the increase of LAMP1 as a result of loss of C9orf72 was reversed by the deletion of CARM1. (F and G) WT, C9orf72-/-, and C9orf72/CARM1 double knockout MEFs were grown under glucose starvation for 16

hours, the autophagic digestion of LDs was examined by immunostaining lysosomes with LAMP1 and co-labeling LDs with BODIPY. The number of BODIPY and LAMP1 double positive puncta per cell was quantified. 30-40 cells in each group from 3 independent experiments were statistically analyzed. Data are presented as mean ± SEM; *p < 0.05, **p < 0.01, ***p < 0.001, ****p < 0.0001.

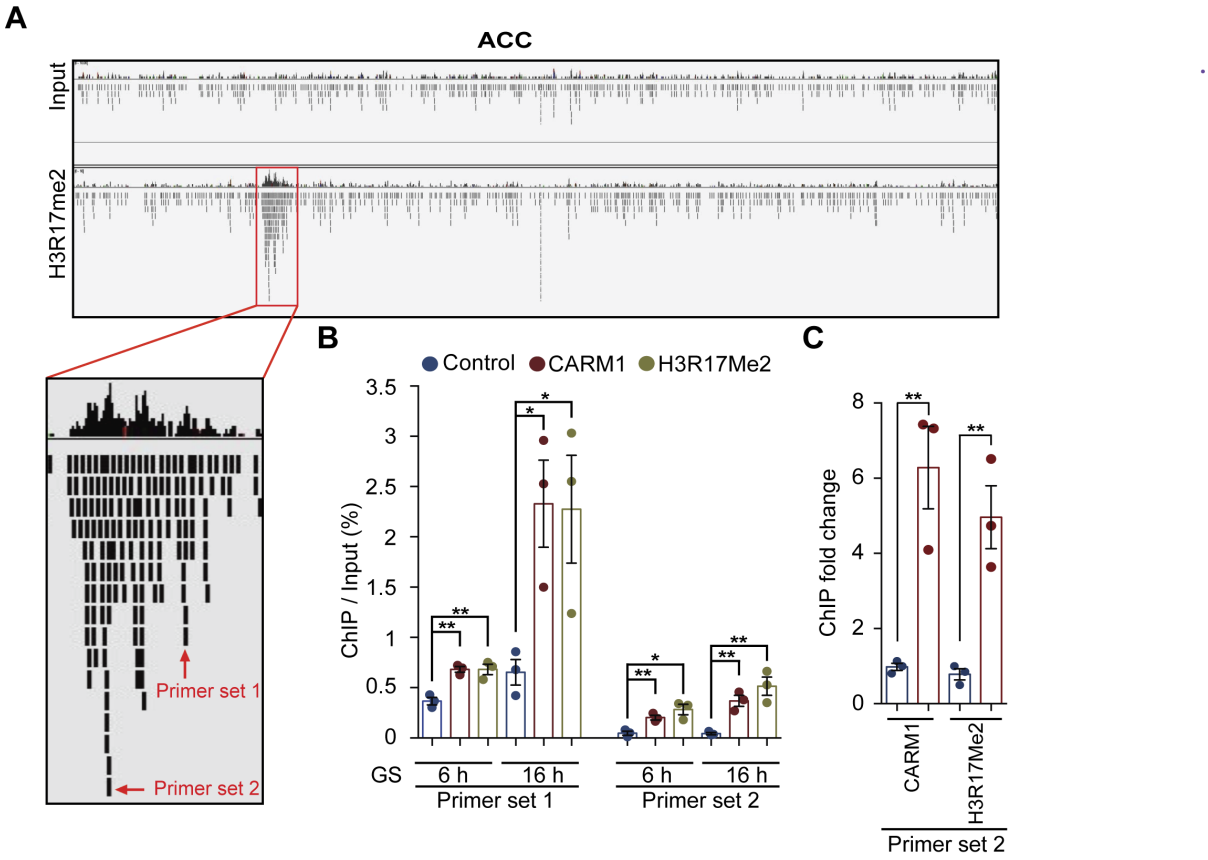


**Supplemental Figure S6. Enrichment of CARM1 and H3R17me2 on the promoter of ACC.**

(A) Analysis of a previously reported ChIP-seq dataset data (Shin et al., 2016), which was obtained from MEFs under glucose starvation conditions, shows that H3R17me2 is enriched at the promoter of the mouse ACC gene. Two primer sets targeting to different sites in the ChIP-seq peak were designed to confirm the enrichment using ChIP-qPCR. (B) MEFs were grown under glucose starvation conditions for 6 hours and 16 hours, and then subjected to ChIP-qPCR using antibodies against CARM1, H3R17me2, or an IgG control. The results using the two different primer sets confirmed the enrichment of CARM1 and H3R17me2 at the promoter of ACC. The ratio of ChIP to input signals is shown. n=3. (C and D) WT and C9orf72-/- MEFs were grown with glucose free medium for 6 hours. Similar to the results in

Fig. 6l using primer set 1, the enrichment of CARM1 and H3R17me2 on the promoter of ACC in each group was confirmed by ChIP-qPCR using anti-CARM1 and anti-H3R17me2 antibodies, respectively, and primer set 2. n=3. The ChIP signals of CARM1 or H3R17me2 relative to IgG are shown. Data are presented as mean ± SEM; *p < 0.05, **p < 0.01.

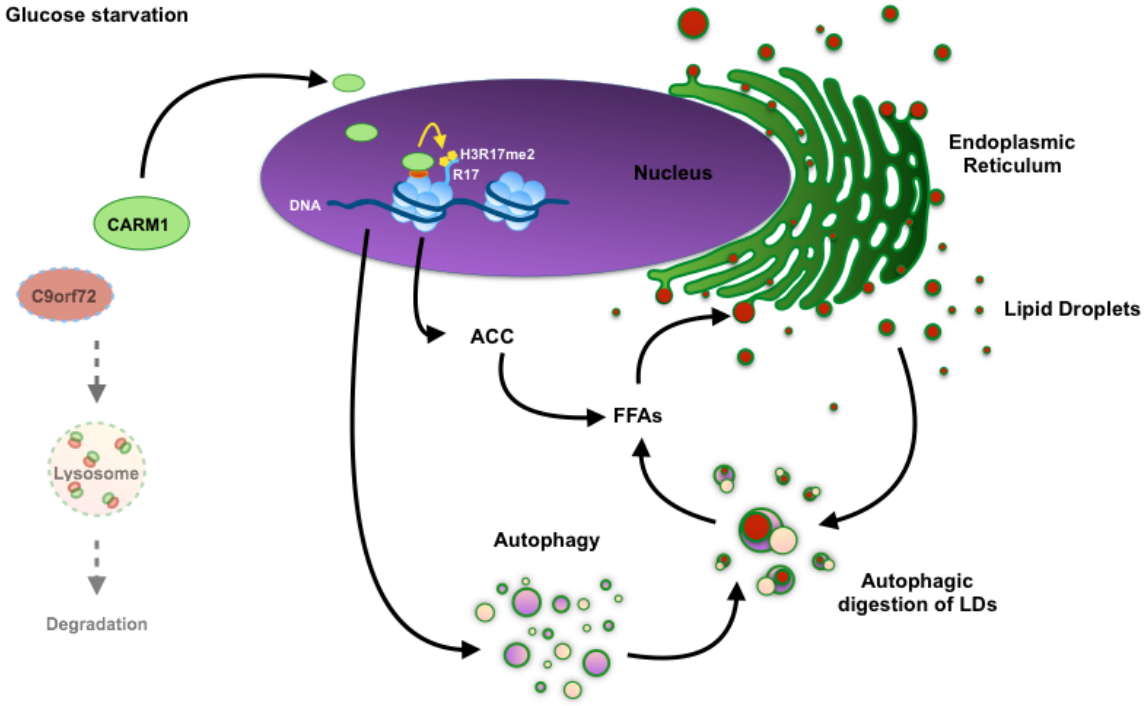


**Supplemental Figure S7. Graphical summary for the C9orf72-CARM1 signaling cascade.**

C9orf72 binds CARM1 and recruits it to the lysosome for degradation, a process that is enhanced under glucose starvation conditions. In the absence of C9orf72, CARM1 is no longer recruited to the lysosome but instead accumulates in the nucleus and regulates gene expression as an arginine methyltransferase for histone and a transcriptional co-activator. CARM1 activates the expression of ACC, a rate-limiting enzyme in FA *de novo* synthesis. CARM1 also positively regulates the autophagic process that digests LDs and increases lipid metabolism. This signaling cascade represents previously unknown pathway in regulating lipid mobilization under nutrient stress in the cell.

## Supplemental Table S1. The list of C9orf72 binding proteins identified in the proteomic analysis.

| Gene symbol | Protein description | Refseq_Protein accession | Σ# Unique Peptides | Σ# PSMs | C9orf72/control: Heavy/Light |
|---|---|---|---|---|---|
| **C9orf72** | **protein C9orf72 isoform a** | **NP_060795.1** | **15** | **355** | **14.10** |
| SMCR8 | Smith-Magenis syndrome chromosomal region candidate gene 8 protein | NP_658988.2 | 3 | 5 | 11.2 |
| WDR41 | WD repeat-containing protein 41 | NP_060738.2 | 5 | 9 | 5.85 |
| FAF2 | FAS-associated factor 2 | NP_055428.1 | 4 | 7 | 5.80 |
| DNAJA2 | dnaJ homolog subfamily A member 2 | NP_005871.1 | 4 | 11 | 5.48 |
| DNAJC11 | dnaJ homolog subfamily C member 11 | NP_060668.2 | 3 | 7 | 5.47 |
| SLC25A6 | ADP/ATP translocase 3 | NP_001627.2 | 3 | 38 | 5.03 |
| AFG3L2 | AFG3-like protein 2 | NP_006787.2 | 3 | 5 | 4.96 |
| **CARM1** | **histone-arginine methyltransferase CARM1** | **NP_954592.1** | **6** | **26** | **4.87** |
| TUBA1A | tubulin alpha-1A chain isoform 2 | NP_001257329.1 | 4 | 83 | 4.85 |
| SLC25A3 | phosphate carrier protein, mitochondrial isoform b precursor | NP_998776.1 | 3 | 6 | 4.70 |
| SLC25A3 | basigin isoform 2 | NP_940991.1 | 3 | 12 | 4.62 |
| PHGDH | D-3-phosphoglycerate dehydrogenase | NP_006614.2 | 9 | 25 | 4.55 |
| SND1 | staphylococcal nuclease domain-containing protein 1 | NP_055205.2 | 3 | 5 | 4.50 |
| MARCKS | myristoylated alanine-rich C-kinase substrate | NP_002347.5 | 3 | 6 | 4.33 |
| FARSA | phenylalanine--tRNA ligase alpha subunit | NP_004452.1 | 4 | 7 | 4.32 |
| ACSL3 | long-chain-fatty-acid--CoA ligase 3 | NP_004448.2 | 5 | 10 | 4.21 |
| PPP2R1A | serine/threonine-protein phosphatase 2A 65 kDa regulatory subunit A alpha isoform | NP_055040.2 | 7 | 18 | 4.17 |
| AIFM1 | apoptosis-inducing factor 1, mitochondrial isoform 2 precursor | NP_665811.1 | 6 | 17 | 4.00 |
| RPS3 | 40S ribosomal protein S3 isoform 1 | NP_001243731.1 | 9 | 32 | 3.95 |
| TUFM | elongation factor Tu, mitochondrial precursor | NP_003312.3 | 4 | 9 | 3.76 |
| TUBB4B | tubulin beta-4B chain | NP_006079.1 | 3 | 180 | 3.75 |
| HSPA8 | heat shock cognate 71 kDa protein isoform 1 | NP_006588.1 | 14 | 119 | 3.72 |
| ST13 | hsc70-interacting protein | NP_003923.2 | 4 | 10 | 3.66 |
| GARS | glycine--tRNA ligase precursor | NP_002038.2 | 8 | 19 | 3.60 |
| FASN | fatty acid synthase | NP_004095.4 | 5 | 9 | 3.54 |
| TRAP1 | heat shock protein 75 kDa, mitochondrial isoform 2 | NP_001258978.1 | 4 | 18 | 3.51 |
| STIP1 | stress-induced-phosphoprotein 1 | NP_006810.1 | 4 | 8 | 3.40 |
| ATP5A1 | ATP synthase subunit alpha, mitochondrial isoform a precursor | NP_001001937.1 | 7 | 14 | 3.28 |
| MCM7 | DNA replication licensing factor MCM7 isoform 1 | NP_005907.3 | 4 | 10 | 3.26 |
| SLC25A13 | calcium-binding mitochondrial carrier protein Aralar2 isoform 2 | NP_055066.1 | 3 | 7 | 3.19 |
| TRIM28 | transcription intermediary factor 1-beta | NP_005753.1 | 3 | 9 | 3.17 |
| TCP1 | T-complex protein 1 subunit alpha isoform a | NP_110379.2 | 11 | 33 | 3.15 |
| ANKFY1 | ankyrin repeat and FYVE domain-containing protein 1 isoform 1 | NP_057460.3 | 5 | 10 | 3.06 |
| STK38 | serine/threonine-protein kinase 38 | NP_009202.1 | 6 | 21 | 3.06 |
| PSMA4 | proteasome subunit alpha type-4 isoform 1 | NP_002780.1 | 4 | 7 | 3.02 |
| SPIN1 | spindlin-1 | NP_006708.2 | 3 | 11 | 2.95 |
| CCT6A | T-complex protein 1 subunit zeta isoform b | NP_001009186.1 | 5 | 14 | 2.93 |
| CCT5 | T-complex protein 1 subunit epsilon | NP_036205.1 | 12 | 60 | 2.90 |
| PGAM5 | serine/threonine-protein phosphatase PGAM5, mitochondrial isoform 3 | NP_612642.2 | 2 | 2 | 2.90 |
| CCT4 | T-complex protein 1 subunit delta isoform a | NP_006421.2 | 14 | 46 | 2.80 |

## Supplemental Table S2. The list of patient tissues and cells.

**Supplemental Data Table 2 The list of patient tissues and cells.**

| Tissues/Cells | Sample ID | Patient ID | Source | R/G | Age at sampling/ Age at DOD | Diagnosis | C9orf72 | Region |
|---|---|---|---|---|---|---|---|---|
| Human spinal cord tissues | SC1 | 90018 | VABBB | /M | -/82 | CTL | No | SC-C |
| | SC2 | 90015 | VABBB | /M | -/66 | CTL | No | SC-C |
| | SC3 | 103 | TALS | W/M | -/22 | CTL | No | SC-C |
| | SC4 | 95 | TALS | /M | -/72 | CTL | No | SC-C |
| | SC5 | 92 | TALS | W/M | -/72 | fALS* | Yes | SC-C |
| | SC6 | 88 | TALS | W/M | -/59 | FTD/sALS | Yes | SC-C |
| | SC7 | 38 | TALS | W/F | -/34 | sALS | Yes | SC-C |
| Human B lymphocytes | BL1 | ND03052 C | NINDS | W/F | 56/- | CTL | No | Blood |
| | BL2 | ND11549 A | NINDS | W/F | 67/- | CTL | No | Blood |
| | BL3 | ND10123 A | NINDS | W/M | 55/- | ALS | Yes | Blood |
| | BL4 | ND12421 A | NINDS | W/F | 56/- | ALS | Yes | Blood |
| Human iPSCs | MN1 | NDS00242 | NINDS | W/F | 49/- | CTL | No | - |
| | MN2 | NDS00241 | NINDS | W/M | 36/- | CTL | No | - |
| | MN3 | NDS00247 | NINDS | W/M | 60/60 | FTD/ALS | Yes | - |
| | MN4 | NDS00239 | NINDS | W/F | 64/65 | ALS# | Yes | - |

Abbreviations: ALS (amyotrophic lateral sclerosis), fALS (familial amyotrophic lateral sclerosis), sALS (sporadic amyotrophic lateral sclerosis), FTD (Frontotemporal Degeneration), CTL (control), W (white), M (male), F (female), DOD (date of death), TALS (TargetALS Postmortem Tissue Core), VABBB (VA biorepository brain bank), NINDS (National Institute of Neurological Disease and Stroke), SC-C (spinal cord cervical). *The patient's son was diagnosed with FTD. #The patient's father was diagnosed with dementia.